Communication

High Mobility Single-Crystal Field-Effect Transistors from Bisindoloquinoline Semiconductors

Eilaf Ahmed, Alejandro L. Briseno, Younan Xia, and Samson A. Jenekhe

J. Am. Chem. Soc., **2008**, 130 (4), 1118-1119 • DOI: 10.1021/ja077444g

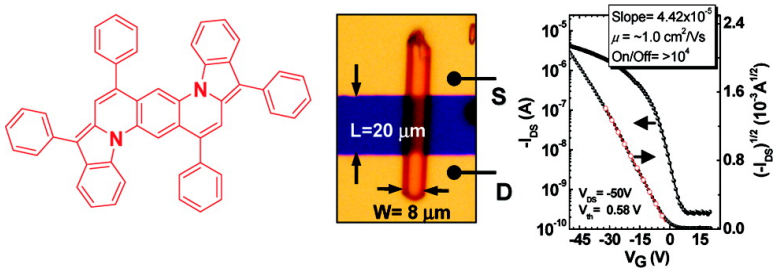

More About This Article

Additional resources and features associated with this article are available within the HTML version:

- Supporting Information
- Links to the 3 articles that cite this article, as of the time of this article download
- Access to high resolution figures
- Links to articles and content related to this article
- Copyright permission to reproduce figures and/or text from this article

View the Full Text HTML

J|A|C|S
COMMUNICATIONS

Published on Web 01/03/2008

High Mobility Single-Crystal Field-Effect Transistors from Bisindoloquinoline Semiconductors

Eilaf Ahmed,[†] Alejandro L. Briseno,[†] Younan Xia,[†] and Samson A. Jenekhe*[,†,‡]

Departments of Chemistry and Chemical Engineering, University of Washington, Seattle, Washington 98195-1750

Received September 26, 2007; E-mail: jenekhe@u.washington.edu

Organic semiconductors are of broad fundamental and technological interests.[1−8] They are being explored in device applications such as organic field-effect transistors (OFETs), photovoltaic cells, and light-emitting diodes.[1−8] There is a great interest in understanding charge transport mechanisms and in establishing the underlying structure−property relationships in organic semiconductors.[1−8] Although there is a vast literature on small-molecule and oligomer-based semiconductors, such as oligoacenes and oligothiophenes, the design and synthesis of new materials are necessary to enable "molecular engineering" of electronic properties for realizing high-performance organic electronics.[1−8]

A common method for investigating the intrinsic charge transport properties of organic semiconductors is the single-crystal field-effect transistor.[7] Organic single crystals are free of grain boundaries or molecular disorder and are routinely employed as tools for determining the performance limitations of semiconductor materials.[1c,6] We report herein high-performance single-crystal transistors fabricated from a novel heptacyclic organic semiconductor bearing nitrogen heteroatoms and a planar molecular backbone, tetraphenylbis(indolo{1,2-a})quinoline (**TPBIQ**). The newly synthesized and crystallized **TPBIQ** exhibits a slipped $\pi-\pi$ stacking, a low ionization potential, and field-effect mobilities as high as 1.0 $cm^2/V\cdot s$.

The synthetic pathway to the heptacyclic bis(indolo{1,2-a})-quinolines (**1**) involved an intramolecular cyclization reaction on anthrazoline derivatives (**4**) as shown in Scheme 1. This new class of heteroaromatic semiconductors contains seven fused rings, including five hexagons and two pentagons. Our group has reported the structure and properties of derivatives of compound **4** which do not exhibit any significant $\pi-\pi$ interactions.[8] Utilizing an intramolecular cyclization reaction on the tricyclic **4**, we anticipated a more conjugated and planar heteroaromatic framework for charge transport in the heptacyclic **1**. The intramolecular cyclization of **4** proceeds in the presence of anhydrous DDQ to afford **TPBIQ** in 32% yield. Tetraphenylanthrazoline **4** was synthesized from the diphenylacetone **3** and 2,5-dibenzoyl-1,4-phenylenediamine **2** in a high yield (75%) via a Friedlander condensation using diphenylphosphate (DPP) as an acid catalyst.[9] 2,5-Dibenzoyl-1,4-phenylenediamine **2** was synthesized according to the literature.[10] **TPBIQ** was twice recrystallized from a 1:1 THF/MeOH solvent mixture and is soluble in common organic solvents such as chloroform, benzene, and toluene. ^{1}H NMR, high-resolution mass spectrometry, and X-ray crystallography confirmed the structure of **TPBIQ**. For example, the singlet resonance at δ 5.81 ppm due to the methine proton in precursor **4** was completely absent in the ^{1}H NMR spectrum of **TPBIQ**. A single molecular ion peak at 658.91 *m*/*z*, which is expected from the calculated molecular weight was observed in the high-resolution mass spectrum. Thermogravimetric analysis showed a high onset decomposition temperature

Scheme 1. The Synthesis of Bis(indolo{1,2-a})quinolines

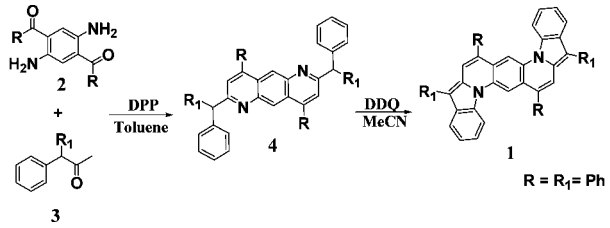

(T_d) at 427 °C. A sharp melting peak (T_m) at 375 °C was observed by differential scanning calorimetry. The high T_d and T_m of **TPBIQ** indicate its excellent thermal stability.

Cyclic voltammetry was performed in benzene/acetonitrile (3:1 v/v) solution and on thin films. **TPBIQ** shows a reversible oxidation and quasi-reversible reduction in solution (Supporting Information). The half-wave oxidation ($E_{1/2}^{ox}$) and reduction ($E_{1/2}^{red}$) potentials were 0.79 and −1.80 V (vs SCE), respectively. From the observed redox potentials, the ionization potential (IP) or HOMO level and electron affinity (EA) or LUMO level of **TPBIQ** were estimated[11] to be ∼5.19 and 2.60 eV, respectively. Cyclic voltammetry of **TPBIQ** thin films gave onset oxidation and reduction potentials of 0.74 and −1.61 V (vs SCE), respectively, from which we derived a solid-state IP (or HOMO level) of 5.14 eV and an EA of 2.79 eV.[11] The estimated electrochemical band gap (E_g^{el}) is thus 2.35 eV.

The optical absorption and photoluminescence (PL) spectra of **TPBIQ** in dilute (7.5×10^{-6} M) chloroform solution are shown in Figure 1. Both spectra show vibronic structure with the 0−0 transition in the absorption at 537 nm, while the orange PL has an emission maximum at 561 nm. Absorption and PL emission spectra of vacuum-deposited thin films (∼65 nm thick) similarly showed vibronic structure with onset absorption at 583 nm and absorption maximum at 517 nm. The solid-state optical band gap (E_g^{opt}) calculated from the onset absorption is 2.13 eV. The PL emission of the thin films was orange-red and had a maximum at 625 nm.

Single crystals of **TPBIQ** were grown by physical vapor transport sublimation. X-ray crystallography was performed to investigate the solid-state packing and the intermolecular interactions in the new organic semiconductor. **TPBIQ** forms a monoclinic *c* lattice, with a space group *C*2/*c* and the unit cell dimensions of a = 18.8707(11) Å, b = 13.9159(8) Å, c = 12.4345(7) Å, $\alpha = 90°$, β = 95.581°(3), and $\gamma = 90°$. The crystal structure reveals that the seven fused rings are relatively planar and that the phenyl rings at C_7 and C_{10} have a twist angle of 42 and 50°, respectively (Figure 2A). Figure 2B shows a slipped face-to-face π-stacking along the *c*-axis. In addition, the shortest distance between the molecules is inclined to the *c*-axis by ca. 32°. The shortest intermolecular spacing of N1−N1′ between adjacent molecules is 3.47 Å. The shortest intermolecular distance between two molecular planes is 3.30 Å as shown in Figure 2B. This suggests that charge transport is likely to be most efficient along the crystallographic *c*-axis due to the

[†] Department of Chemistry.
[‡] Department of Chemical Engineering.

10.1021/ja077444g CCC: $40.75

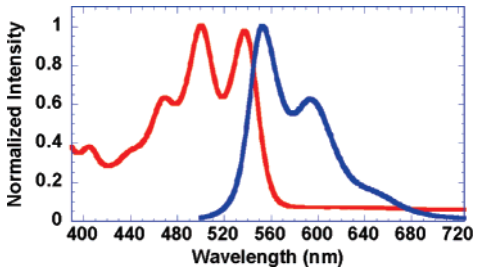

Figure 1. Absorption and photoluminescence (PL) spectra of **TPBIQ** solution in chloroform.

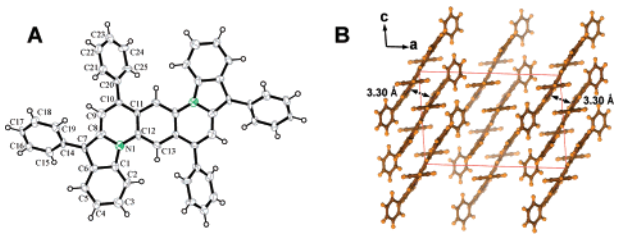

Figure 2. (A) ORTEP plot of **TPBIQ** and (B) view down the crystallographic *b*-axis with indicated intermolecular contacts of 3.30 Å.

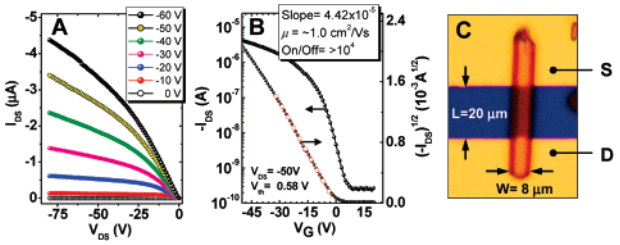

Figure 3. (A) Output and (B) transfer characteristics of a **TPBIQ** single-crystal transistor. (C) An optical micrograph of the single-crystal device corresponding to the data in Figure A,B.

excellent intermolecular overlap of electronic wave functions. Furthermore, the molecular packing of **TPBIQ** molecules along the *a*-axis of the crystal structure indicates that there is no π-electron overlap. This type of intermolecular organization is reminiscent of the molecular packing in rubrene single crystals which give rise to anisotropic charge transport.[7b]

We examined the charge transport properties of **TPBIQ** by directly growing single crystals onto source-drain electrodes by physical vapor transport.[7a] Transistor arrays were fabricated by conventional photolithography, and Cr/Au was employed to define source-drain electrodes. Figure 3A,B shows the p-channel electrical characteristics of the single-crystal device shown in Figure 3C. The output characteristics show well-resolved saturation currents for several gate voltage values. Figure 3B shows a plot of both the log and the square root of drain current as a function of gate voltage. We calculated a field-effect mobility of 1.0 cm^2/V·s in the saturation region, on/off ratios greater than 10^4, and a relatively low switch-on voltage of 0.58 V at $V_{DS} = -50$ V. Field-effect mobilities from at least eight single-crystal devices ranged from 0.3 to 1.0 cm^2/V·s. We emphasize that no surface treatment was administered on our device substrates and that crystals were randomly grown across source-drain electrodes. However, measurements were only performed on devices that contained one single-crystal bridging the source-drain electrodes, and optical micrographs (Figure 3C) were recorded to accurately measure W/L values for mobility calculations. Finally, the growth direction of the crystal was determined to be along the [001] direction. This long axis was identified as the *c*-axis and also the short $\pi-\pi$ stacking direction. Therefore, the carrier mobility of our device from Figure 3C was measured along *c*-axis direction.

In conclusion, we have synthesized a new class of heteroaromatic semiconductors via an intramolecular cyclization that results in a novel heptacyclic π-conjugated framework showing a planar geometry with excellent $\pi-\pi$ stacking. Single-crystal transistors yielded mobilities as large as 1.0 cm^2/V·s. In addition, the high stability from electrochemical and thermal measurements suggests that this new class of heteroaromatic semiconductors is an excellent candidate for further studies in organic electronics. Ongoing work is exploring the synthesis and properties of derivatives of compound **1** with different R groups.

Acknowledgment. We acknowledge support from NSF (CTS-0437912 and DMR-0120967) and AFOSR (F49620-03-1-0162). A.L.B. acknowledges the Bell Labs Graduate Fellowship. Y.X. acknowledges support from the David and Lucile Packard Foundation. We thank W. Kaminsky for determining the crystal structure of **TPBIQ**.

Supporting Information Available: Detailed synthetic procedures, additional data and X-ray crystallographic data in CIF format. This material is available free of charge via the Internet at http://pubs.acs.org.

References

(1) (a) Anthony, J. E. *Chem. Rev.* **2006**, *106*, 5028. (b) Bendikov, M.; Wudl, F.; Perepichka, D. F. *Chem. Rev.* **2004**, *104*, 4891. (c) Coropceanu, V.; Cornil, J.; da Silva Filho, D. A.; Olivier, Y.; Silbey, R.; Brédas, J.-L. *Chem. Rev.* **2007**, *107*, 926. (d) See special issue on organic electronics: *Chem. Mater.* **2004**, *16*, 4381.

(2) (a) *Electronic Materials: The Oligomer Approach*; Müllen, K., Wegner, G., Eds.; Wiley-VCH: Weinheim, Germany, 1998. (b) Pope, M.; Swenberg, C. E. *Electronic Processes in Organic Crystals*; Oxford University Press: New York, 1999.

(3) (a) Katz, H. E.; Bao, Z.; Gilat, S. L. *Acc. Chem. Res.* **2001**, *34*, 359. (b) Otsubo, T.; Aso, Y.; Takimiya, K. *J. Mater. Chem.* **2002**, *12*, 2565. (c) Merlo, J. A.; Newman, C. R.; Gerlach, C. P.; Kelley, T. W.; Muyres, D. V.; Fritz, S. E.; Toney, M. F.; Frisbie, C. D. *J. Am. Chem. Soc.* **2005**, *127*, 3997.

(4) (a) Moon, H.; Zeis, R.; Borkent, E.-J.; Besnard, C.; Lovinger, A. J.; Siegrist, T.; Kloc, Ch.; Bao, Z. *J. Am. Chem. Soc.* **2004**, *126*, 15322. (b) Boudreault, P. L. T.; Wakim, S.; Blouin, N.; Simard, M.; Tessier, C.; Tao, Y.; Leclerc, M. *J. Am. Chem. Soc.* **2007**, *129*, 9125. (c) Facchetti, A.; Yoon, M. H.; Stern, C. L.; Hutchison, G. R.; Ratner, M. A.; Marks, T. J. *J. Am. Chem. Soc.* **2004**, *126*, 13480.

(5) (a) Curtis, M. D.; Cao, J.; Kampf, J. W. *J. Am. Chem. Soc.* **2004**, *126*, 4318. (b) Babel, A.; Jenekhe, S. A. *J. Am. Chem. Soc.* **2003**, *125*, 13656.

(6) Mas-Torrent, M.; Hadley, P.; Bromley, S. T.; Ribas, X.; Tarres, J.; Mas, M.; Molins, E.; Veciana, J.; Rovira, C. *J. Am.Chem. Soc.* **2004**, *126*, 8546.

(7) (a) Briseno, A. L.; Mannsfeld, S. C. B.; Ling, M.; Liu, S.; Tseng, R. J.; Reese, C.; Roberts, M.; Yang, Y.; Wudl, F.; Bao, Z. *Nature* **2006**, *444*, 913. (b) Sundar, V. C.; Zaumseil, J.; Podzorov, V.; Menard, E.; Willett, R. L.; Someya, T.; Gershenson, M. E.; Rogers, J. A. *Science* **2004**, *303*, 1644. (c) de Boer, R. W. I.; Gershenson, M. E.; Morpurgo, A. F.; Podzorov, V. *Phys. Status Solidi A* **2004**, *201*, 1302. (d) Gershenson, M. E.; Podzorov, V.; Morpurgo, A. F. *Rev. Mod. Phys.* **2006**, *8*, 973.

(8) Tonzola, C. J.; Alam, M. M.; Kaminsky, W.; Jenekhe, S. A. *J. Am. Chem. Soc.* **2003**, *125*, 13548.

(9) (a) Agrawal, A. K.; Jenekhe, S. A. *Macromolecules* **1991**, *24*, 6806. (b) Agrawal, A. K.; Jenekhe, S. A. *Macromolecules* **1993**, *26*, 895.

(10) Imai, Y.; Jonson, E. F.; Katto, T.; Kurihara, M.; Stille, J. K. *J. Polym. Sci.: Polym. Chem. Ed.* **1975**, *13*, 2233.

(11) We used the relations, $E_{1/2}^{ox} + 4.4 =$ IP and $E_{1/2}^{red} + 4.4 =$ EA; see: Kulkarni, A. P.; Tonzola, C. J.; Babel, A.; Jenekhe, S. A. *Chem. Mater.* **2004**, *16*, 4556.

JA077444G